

# Manufacturing Epoxy and Polyurethane-based Artificial Stones from Waste Glass of Colorless Beverage Packaging

Gabriela Nunes Sales Barreto<sup>a\*</sup> , José Lucas Decoté de Carvalho Lírio<sup>a</sup>,

Maria Luíza Pessanha Menezes Gomes<sup>a</sup> , Elaine Aparecida Santos Carvalho<sup>a</sup> ,

Henry Alonso Colorado Lopera<sup>b</sup>, Carlos Mauricio Fontes Vieira<sup>a</sup> 

<sup>a</sup>Universidade Estadual do Norte Fluminense Darcy Ribeiro (UENF), Laboratório de Materiais Avançados, Av. Alberto Lamego, 2000, Campos dos Goytacazes, RJ, Brasil.

<sup>b</sup>Univeristy of Antioquia (UdeA), CCComposites; Cl. 67 #53-108, 050010, Medellín, Antioquia, Colombia.

Received: January 09, 2023; Revised: July 31, 2023; Accepted: September 14, 2023

Novel civil construction materials based on waste can be an optimal alternative for waste management, reducing its improper disposal while engaging an otherwise discarded material as a raw material in other production processes. This research's main objective was to develop and characterize two novel artificial stones based on waste glass from bottles and aggregated with epoxy resin (ASG-EP) and polyurethane resin (ASG-PU) from castor oil, respectively, as well as the comparison of the two developed materials. Plates were manufactured with 15% of epoxy or 15% polyurethane resins and 85% of waste glass from bottles. The mixture was molded with a process of 6Hz vibration, 600mmHg of vacuum, and hot compaction at 90°C for EP and 80°C for PU. Results evidenced that the development of ASGs based on waste glass from bottles is technically and economically viable.

**Keywords:** *Artificial stone, Polymeric matrices, Waste Glass, Polyurethane Resin, Epoxy Resin.*

## 1. Introduction

The fast development of the worldwide economy, urbanization, populace and standard of living has expanded waste generation, which increased the utilization of natural resources as well as the management of economic additional costs. Deficient waste management can lead to natural defilement and health dangers. Waste represents poor handling of resources, being an image of an inefficient modern society<sup>1</sup>.

Research efforts worldwide are focusing on improving solid waste management, driven by the need to recover waste and prevent improper disposal<sup>2</sup>. One promising alternative is to use waste as a sub-product in the development of novel civil construction materials, as this industry is rapidly growing and constantly demands raw materials that account for 75% of natural resource waste<sup>3</sup>. By adopting waste reuse, the civil construction sector can meet sustainable development parameters and save on raw material costs.

Especially, the stone sector is enlarging its business and production, with stone operations refining themselves, which enhances the production rate thus jeopardizing the environment with its amount of non-biodegradable waste swells. Stone wastes have the potential to impair water, soil, and population health, and, if dumped into landfills. This material is put into better use if it is employed in the manufacturing of other products, such as ceramic<sup>4-6</sup>, cement composites<sup>7-9</sup>, and other materials<sup>10</sup> leading to economic and sustainable advantages<sup>11</sup>.

Artificial stones, also known as engineered, composite, or polymer concrete, are made by crushing and aggregating 90-96% natural materials with polymer matrices. This creates a mixed paste that is hot compacted under vacuum and vibration with resins and additives. The result is a dense, mechanically strong, and aesthetically appealing stone plate that is available in different sizes. This material is used in various applications such as floors, walls, and countertops, offering environmental and commercial value by reusing stone waste and reducing wrongly disposed waste. The controlled production process originates a material with superior mechanical properties and therefore, the market for artificial stones has been growing significantly in the past 20 years<sup>12,13</sup>.

Numerous studies have explored the use of waste as a substitute for aggregates in artificial stones, which are agglomerated by resins like epoxy<sup>14,15</sup> or polyester<sup>16,17</sup>. These studies have demonstrated the potential for producing materials with excellent properties suitable for manufacturing by industries. However, the use of petroleum-based polymers contradicts the concept of sustainability due to their slow degradation and by-product production. In this study, a vegetable-based resin, polyurethane from castor oil, was used to address this issue. Although polyurethane resin has lower mechanical strength and limited ductility compared to synthetic polymers, using vegetable-based polymers has the potential to create a more sustainable material<sup>18</sup>.

The goal of this project is to develop and analyze an artificial stone composed of waste glass from beverage bottles and polyurethane resin derived from castor oil.

\*e-mail: [gabibarroto93@gmail.com](mailto:gabibarroto93@gmail.com)

The performance of this material will be compared to stones made with the same composition of glass waste but with epoxy resin, to assess its technical feasibility. This work aims to create a sustainable and commercially viable material for use in civil construction that aligns with the principles of sustainable development.

## 2. Materials and Methods

### 2.1. Materials

The authors collected waste glass from colorless beverage packaging in local bars and supermarkets in Campos dos Goytacazes, Rio de Janeiro, Brazil. Two types of resins were utilized as polymeric matrices in this study: vegetable-based polyurethane (PU) derived from castor oil and epoxy resin (MC130) of diglycidyl ether bisphenol A (DGEBA) type. The polyurethane resin, with a density of 1.08 g/cm<sup>3</sup>, was obtained from Imperverg, a Brazilian company, and consists of a prepolymer (component A) and a polyol (component B) that were hot mixed in a 1:1.18 proportion. The epoxy resin (density: 1.15 g/cm<sup>3</sup>) and its hardener, TETA (Triethylenetetramine - FD 129), were supplied by Epoxyfiber, a Brazilian company.

### 2.2. Methods

Colorless glass beverage bottles were collected and cleaned with soap and water, air-dried, and then broken into smaller pieces using a hammer. These pieces were further crushed into finer particles using a jaw crusher. For waste glass chemical composition identification, XRF analysis was conducted using a Bruker S8 Tiger X-Ray fluorescence spectrometer, which uses a rhodium (Rh) anode composition, with a maximum power of 1 kW, a voltage range of 20-50 kV, and a current range of 5-50 mA.

The waste particles were sieved to sort them into three sizes: coarse (2.000 - 1.190 mm), medium (1.190 - 0.149 mm), and fine (< 0.149 mm). The most densely packed mixture of these three sizes was determined by testing ten (10) different mixtures according to the ternary diagram of the Simplex-Lattice Design represented in Figure 1, according to Brazilian standard NBR MB-3388<sup>19</sup>. This is the same procedure that the artificial stone industry uses to decide the particle size composition of its raw materials when manufacturing artificial stones for the market.

Mixtures were put in a 1,013.24 cm<sup>3</sup> steel vessel coupled to a 10 kg weight under 60 Hz. After 10 minutes of vibration, the mixtures were weighted. For each of the 10 mixtures, the procedure was repeated three times, to guarantee the statistical reliability of the results.

It's imperative to determine the highest packing mixture to select, amongst the 10 possibilities, the composition that would provide the stone with better properties, as the highest packing mixture would produce a final product with a lower void index.

Using Microsoft Excel software, the results of the best package test underwent statistical treatment through analysis of variance (ANOVA) using a completely randomized design (CRD) with a significance level set at  $p \leq 0.05$ , to verify the statistical significance of the data. Upon validating the statistical difference, a Tukey test ( $p \leq 0.05$ ) was applied to

confirm the mixture that yielded the best results, which was chosen for producing the engineered stone plates since, as explained above, would provide an artificial stone with as optimal mechanical properties as possible.

The real density of the mixture was determined by the pycnometer method, and together with the vibrated density information of the best package mixture, the minimum amount of resin (MAR)<sup>20</sup> required for producing the ASG (Artificial Stone based on Glass) plates was calculated through the volume void index (VI) through Equation 1:

$$VI\% = 1 - \left( \frac{\text{particles vibrate density}}{\text{waste glass mixture real density}} \right) * 100 \quad (1)$$

The minimum amount of resin (MAR), represented by the amount of resin enough to fill these volume void index, were then, calculated through Equation 2:

$$MAR\% = \frac{VI\% * \rho_{resin}}{VI\% * \rho_{resin} + (100 - VI\%)} * \rho_{(\text{highest packed mixture of waste glass})} \quad (2)$$

The density of the highest packed mixture of glass waste was calculated by the pycnometer method.

### 2.3. Artificial stone plates manufacturing

Through vacuum, vibration, and compression method, ASG plates sized 100x100x10mm were manufactured.

The coarse, medium, and fine waste glass particles were weighed and mixed in the proportions indicated by the best-packed mixture test, as will be presented in the Results and Discussion section, and were oven-dried at 100°C for 24 hours. Each stone was mixed with one of the two different types of resins, namely vegetable polyurethane and epoxy + TETA, in the appropriate proportions determined by the MAR, which will be also described in the Results and Discussion section.

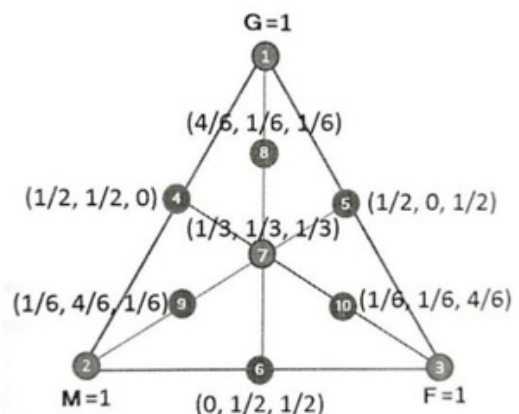


**Figure 1.** Ternary diagram with the Simplex complete cubic model 10 mixtures composition. Proportions of coarse (G), medium (M) and fine (F) particles<sup>15</sup>.

The resulting mixture was placed into a mold connected to a vacuum system with a pressure of 600mmHg and then vibrated for 2 minutes on a table. The mold was then subjected to a hydraulic press at 90°C for epoxy resin and 80°C for polyurethane resin. Once cooled to room temperature, the plate was removed from the mold, sanded, and cut to the desired size for testing.

#### 2.4. Characterization tests

The physical properties of the ASG plates were evaluated based on standard protocols outlined in the ABNT NBR 15845-2<sup>21</sup> guidelines. Therefore, to determine the apparent density, water absorption, and apparent porosity, ten (10) specimens of size 50x50x10mm were tested.

For three-point bend strength, six (6) specimens sized 10x25x100mm were tested on an Instron 5582 Universal testing machine at a load rate of 0.25mm/min, using a 100KN load cell and two-point distance of 80mm as per ABNT NBR 15845-6<sup>22</sup>.

The wear resistance test was carried out using two (2) specimens of size 70x70x30mm, in accordance with the ABNT NBR 12.042<sup>23</sup> standards, using the MAQTEST Amsler machine to measure the thickness loss after a 500 and 1000m wear track.

To evaluate the Izod impact resistance, ten (10) 45° notched specimens of size 62x12x10mm were analyzed following the ASTM D256 standard<sup>24</sup>, using a Pendulum machine branded PANTEC, model XC-50.

Scanning electron microscopy (SEM) equipped with energy dispersive spectroscopy (SEM-EDS) was conducted on the polished and fractured surfaces to evaluate the chemical composition, microstructure, particle interface, and the presence of voids in the samples. The samples were gold-sputtered using a Hummer 6.2 system and analyzed using a JEOL JSM 6700R in a high vacuum mode.

### 3. Results and Discussions

#### 3.1. Determination of the highest packing composition

Table 1 shows the chemical composition of the colorless waste glass from discarded bottles.

In Table 1 it can be observed that the chemical composition of the waste glass from bottles presents a predominance of silica (SiO<sub>2</sub>), sodium oxide (Na<sub>2</sub>O), and calcium oxide aka lime (CaO). It can also be noticed the presence of other compounds, such as alumina (Al<sub>2</sub>O<sub>3</sub>) and alkali metal oxides in smaller quantities.

These results are in accordance with other works that performed XRF analysis in waste glass, such as Xin et al.<sup>25</sup> and Arias-Erazo et al.<sup>26</sup>, which also detected the predominance of silica, sodium oxide, and calcium oxide on their waste glass reused into the production of bricks and concretes, respectively.

It can be noticed that the chemical composition of glass waste is a promising alternative to replace stone aggregates in the development of artificial stone because it shares similar chemical composition with natural dimensioned stones, such as marble and granite. Marble is predominantly composed of calcium oxide (CaO), while granite is predominantly

composed of silicon dioxide (SiO<sub>2</sub>)<sup>27</sup>. Currently, marble and granite wastes are the most common material used in industry to manufacture artificial stones. Therefore, waste glass, which is made of similar raw materials, could be an excellent alternative of waste material that would produce artificial stones with similar mechanical properties to the current ones in the market.

Table 2 shows the vibrate density of the 10 mixtures proposed in Figure 1 for the best-packed test.

As can be seen in Table 2, mixture 7 (1/3 coarse, 1/3 medium, and 1/3 fine particles of waste glass) showed the highest vibrate density, thus being the best-packed mixture and selected for the manufacturing of the ASG plates. The determination of the best-packed mixture is important to evaluate which one of the granulometric compositions would make the stone have the densest structure, with fewer empty spaces that could form voids that could jeopardize its properties.

As the results above represent an average of three vibrate densities found, the data were treated with analysis of variance (ANOVA) considering a completely randomized design (CRD) carried out with a confidence level of 95% (p<0.05), followed by a Tukey test for average contrast, as it can be seen in Table 3.

**Table 1.** Chemical composition of colorless waste glass from beverage bottles by XRF analysis.

Constituent oxides	% wt
SiO <sub>2</sub>	72.16
Na <sub>2</sub> O	13.12
CaO	11.96
Al <sub>2</sub> O <sub>3</sub>	1.49
K <sub>2</sub> O	0.45
MgO	0.24
SO <sub>3</sub>	0.22
ZnO	0.15
Fe <sub>2</sub> O <sub>3</sub>	0.13
TiO <sub>2</sub>	0.09
SrO	0.02
ZrO <sub>2</sub>	<0.01

**Table 2.** Vibrate density of the 10 mixtures proposed for ASGs development.

Mixtures	Vibrate density (g/cm <sup>3</sup> )
1	1.23 ± 0.03
2	1.25 ± 0.02
3	0.95 ± 0.02
4	1.42 ± 0.02
5	1.54 ± 0.07
6	1.45 ± 0.02
7	<b>1.80 ± 0.01</b>
8	1.19 ± 0.04
9	0.98± 0.04
10	1.36± 0.03

Analyzing the results obtained in Tables 2 and 3, it is possible to verify that the studied treatments present no statistical differences, which means that among the 10 mixtures, only one is differentiated. It is worth mentioning the 1,91% coefficient of variation for this test, outlining the reliability of the results. Tukey test was performed to statistically prove the contrast in the vibrated density averages ( $p \leq 0.05$ ), as shown in Table 4.

After performing the Tukey test, it is clear that mixture 7 has the greater vibrated density. Therefore, mixture 7 was chosen as a proportion for the ASGs development and had its real density determined by the pycnometer method as  $2.478 \text{ g/cm}^3$ .

With this data, it was possible to calculate the VI% using Equation 1 and the MAR% using Equation 2. The MAR was calculated as 14,09 and 14,87% for PU and EP resins, respectively. This amount of resin is reasoned to be the minimum amount of matrix needed to fill all the void volume, that is, empty spaces, both interstitial and surficial, from the best-packed mixture.

For that reason, ASG-PU and ASG-EP plates were manufactured with 15%wt of resin and 85% of particles with the composition of mixture 7, representing 1/3 of coarse, 1/3 of medium, and 1/3 of fine waste glass particles.

### 3.2. Physical properties

Table 5 displays the apparent density, water absorption and apparent porosity of ASG-PU and ASG-EP.

As shown in Table 5, the densities of ASG-PU and ASG-EP both are  $2.14 (\pm 0.01) \text{ g/cm}^3$ , which are within the range of density of similar materials, such as Lee et al.<sup>28</sup>, that manufactured artificial stones based on glass and granite wastes varying the parameters of pressure, temperature and vacuum with densities varying between  $2.03$  to  $2.45 \text{ g/cm}^3$ .

Likewise, authors like Agrizzi et al.<sup>29</sup> and Gomes et al.<sup>18</sup>, developed artificial stones with polyurethane resin but different wastes (quartzite and granite) being  $2.22$  and  $2.24 \text{ g/cm}^3$  dense, respectively. It confirms that both ASG-EP and ASG-PU densities are in accordance with similar materials.

Water absorption of ASG-PU and ASG-EP are  $0.88$  and  $0.74\%$ , respectively. As indicated by Chiodi and Rodrigues<sup>30</sup>, which indicates parameters of reference for stones to be applied as a coating, materials ranging from  $0.4$ - $1.0\%$  of water absorption are considered to be of medium quality. Thus, both ASG-EP and ASG-PU can be classified as medium-quality stones to be applied as coatings and it's better to apply them in places with not-so-frequent wetting.

Still, according to Chiodi and Rodrigues<sup>30</sup>, building materials to be used as lining and facing must have porosity from  $1$  to  $3\%$  to be classified as medium-quality materials. As can be seen in Table 5, both ASG-PU and ASG-EP have their porosity value meeting this requirement, also classifying them, according to porosity, as medium-quality building materials for lining and facing.

**Table 3.** ANOVA test results on the CRD of vibrated density ( $p \leq 0.05$ ).

FV	GL	SQ	QM	F
Treatment	9	1,7644	0,1960	153,2445
Waste	20	0,0256	0,0013	
Total	29	1,7900		

Conclusion: calculated  $F <$  tabulated  $F$ , there is no statistical difference.  $F$  tabulated =  $2,39$

**Table 4.** Tukey test for contrasting density averages ( $p \leq 0.05$ ).

Treatment	Average	Tukey test*
7	1.68	A
10	1.63	B
8	1.59	B
6	1.56	BC
5	1.51	CD
9	1.44	DE
4	1.42	E
3	1.25	F
2	1.25	F
1	1.23	F

\*The averages followed by the same letter, in the column, do not differ from each other at 5% probability using the Tukey Test.

**Table 5.** Physical properties of apparent density, water absorption and apparent porosity of the ASG-PU and ASG-EP.

Artificial Stone	Density ( $\text{g/cm}^3$ )	Water absorption (%)	Apparent porosity (%)
ASG-PU	$2.14 \pm 0.01$	$0.88 \pm 0.12$	$1.89 \pm 0.24$
ASG-EP	$2.14 \pm 0.01$	$0.74 \pm 0.01$	$1.59 \pm 0.01$

When comparing with other authors that also produced artificial stones with similar materials, the average water absorption ranges from 0.01-0.67%<sup>14,18,20,28,29</sup>. Regarding porosity, artificial stones that were also developed with vacuum, vibration, and compaction, and similar waste and polymeric materials ranged from 0.3-0.8%<sup>14,18,20,28,29</sup>. Therefore, both the porosity and the water absorption of the ASGs are slightly above the average for artificial stones.

### 3.3. Three-point bend strength

Figure 2 shows stress x strain curves of ASG-PU, ASG-EP, epoxy, and polyurethane resins after 3-point bend strength tests.

By observing Figure 2, one can notice that comparing PU and EP resins with ASG-PU and ASG-EP, the material becomes harder with the addition of particles once the material's flexural modulus increases as the rigid particle content enhances<sup>28</sup>. The mechanical behavior of a material agglomerated by resins is dictated by the interface between the particles and the matrix, better adhesion means better mechanical properties<sup>31</sup>.

Table 6 presents the results of 3-point bend strength for ASG-PU, ASG-EP, epoxy (EP), and polyurethane (PU) resins.

There are more than one standard and parameter for stones to be applied as coatings bending strength. The ABNT NBR 15845-6<sup>22</sup> postulates they should have more than 10MPa bending strength, while ASTM 6880<sup>32</sup> establishes that must be over 8.7MPa. Chiodi and Rodriguez<sup>30</sup> classify stones with bending strength above 20 MPa as high-quality materials for coating applications. Therefore, both ASG-EP and ASG-PU meet all the aforementioned requirements and standards for stones to be applied as coatings in the civil construction industry thus proving the technical feasibility of the developed materials.

Furthermore, ASG-EP has 37.61 MPa of 3-point bend strength, a value way higher than the 20MPa required, denoting its high quality, even though the porosity and water absorption results classified them as medium quality materials, its value did not jeopardize the mechanical strength. When comparing the results of ASG-PU (29.23MPa) with those of ASG-EP, one can notice that ASG-PU's bend strength is lower, which can be attributed to the influence of the matrix into bend strength, once epoxy resin has 93.6MPa flexural strength while polyurethane resin not only has 23MPa but also have a more flexible behavior, as it can be seen in Figure 2.

Gomes et al.<sup>18</sup> also manufactured artificial stones with PU resin based on castor oil and granite wastes by vacuum vibration and compression and their material presented 18MPa of bend strength. The fact that the ASG-PU value of 29.23MPa was almost twice higher than the stone developed by Gomes et al.<sup>18</sup> can be attributed to the fact that this work used a different preparation for the PU resin. The pre-polymer and polyol of the present work were hot mixed, after a 2h heat of both materials, aiming to eliminate bubbles to achieve better properties, which was accomplished.

### 3.4. SEM micrographs of bend-ruptured specimens

Figure 3 (ASG-PU) and Figure 4 (ASG-EP) both display micrographs of surface fracture of the developed engineered stones obtained by SEM.

By observing Figure 3a, it is possible to notice displaced particles or regions of grains detached, which is evidenced by a void where the particle would be placed. This is characteristic of bend-ruptured materials, as the fracture cracks of materials subjected to bending efforts travel across the material grains.

In both Figures 3 and 4, it is possible to notice a low occurrence of pores or cavities, probably due to the process (vacuum, vibration, and compression) employed to develop the artificial stone plates.

The use of vacuum aims to diminish the porosity of the material, since the pressure gradient created by it sucks the resin into the voids, filling them<sup>14</sup>, with the aid of the vibration. The compaction also makes a greater resin/particle adhesion, which can be observed in the images, and has a direct relation to better composite's mechanical properties, according to Debnath et al.<sup>31</sup> and Miller et al.<sup>33</sup>.

Comparing both developed stones, one can see that the stone developed with epoxy resin, ASG-EP, presented a better interaction between the particles and the matrix than the stone developed with polyurethane resin, ASG-PU, which was confirmed by the results of the three-point bend strength test, once ASG-EP had a bending strength higher than ASG-PU.

### 3.5. Wear resistance

Table 7 presents the thickness reduction of ASG-EP and ASG-PU after two specimens were submitted to abrasive wear tests at two running distances, 500 and 1,000 m.

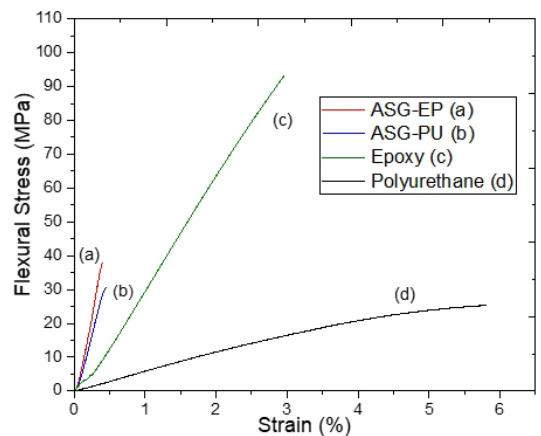


Figure 2. Bend stress x strain curves of ASG-PU, ASG-EP, epoxy, and polyurethane resins.

Table 6. Three-point bend strength resistance of ASG-PU, ASG-EP, epoxy, and polyurethane resins.

	ASG-PU	ASG-EP	EP	PU
<b>Three-point bend strength (MPa)</b>	29.23 ± 1.29	37.61 ± 2.82	93.6±4.7	23 ± 5.3

Even though there are no standards, requirements, or established thickness reduction values for artificial stones, the authors Chiodi and Rodrigues<sup>30</sup> settled technological parameters for artificial stones to be applied on pavements. For pavements to bear low traffic, the wear thickness must be lower than 6mm. For medium traffic, lower than 3 mm. For heavy traffic, lower than 1.5mm.

Following the above guidelines, it is possible to classify both ASG-EP and ASG-PU as artificial stones for pavements to bear medium traffic, owing to the thickness reduction to be less than 3mm on the 1,000m track. ASG-EP has lower thickness loss than ASG-PU, which can be attributed to resin content influence on the material's wear resistance. ASG-PU is based on PU resin, a resin castor oil based, from a natural source with a more flexible, highly crosslinked, and permanent network structure<sup>34</sup>, which can be easily observed in Figure 2 in its stress x strain curve behavior.

In previous work, Barreto et al.<sup>14</sup> developed artificial stones with waste glass mixed up with quartz sand and epoxy resin, and their artificial stone after being subjected to wear resistance tests had a similar thickness loss of 2.86mm in a 1,000m track. On that account, both ASG-EP and ASG-PU thickness loss are in accordance with previous works.

### 3.6. Izod impact resistance

To determine the impact resistance or impact strength of the artificial stones developed, an Izod impact test was performed on both ASG-EP and ASG-PU. Figure 5 displays the results of the Izod impact test for ASG-PU and ASG-EP and the impact resistance data can be seen in Table 8.

**Table 7.** Amsler abrasive wear through thickness reduction of ASG-EP and ASG-EP.

Material	Thickness reduction (mm)	
	500m	1000m
ASG-PU	1.63±0.01	2.87±0.14
ASG-EP	1.20±0.16	2.15±0.21

**Table 8.** Impact resistance of ASG-PU and ASG-EP determined by Izod impact test.

Material	Impact Resistance (J/m)
ASG-PU	15.97± 3.29
ASG-EP	12.70 ± 3.38

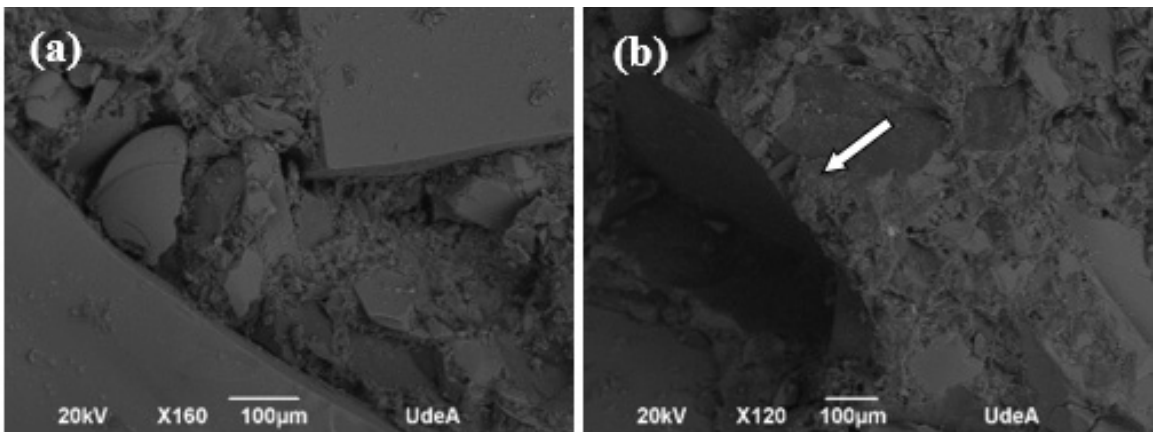


**Figure 3.** ASG-PU SEM micrographs of fractured surface micrographs with 120x.

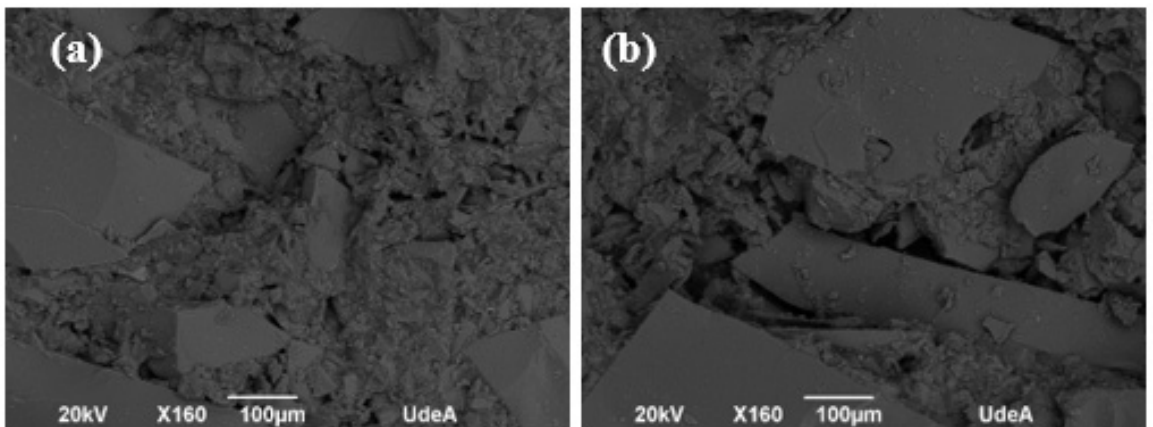


**Figure 4.** ASG-EP SEM micrographs of fractured surface micrographs with 120x.

Izod impact resembles a bending test, where the specimen is tested to determine the amount of energy the material can bear until it ruptures as a function of the thickness. The test is performed until the specimen breaks and the impact resistance is measured in J/m, meaning the energy lost per unit of the specimen's thicknesses<sup>35</sup>.

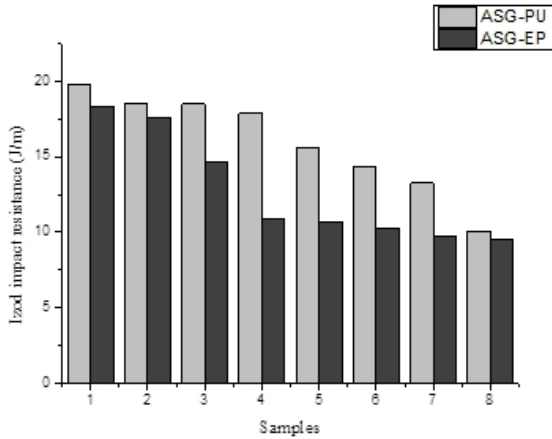


**Figure 5.** Results of Izod impact test for the developed artificial stones: ASG-PU and ASG-EP.

Table 8 shows the impact resistance of ASG-PU and ASG-EP after the impact test.

As shown in Table 8, the impact resistance of ASG-PU ( $14.53 \pm 4.20$  J/m) was higher than the impact resistance of ASG-EP ( $12.70 \pm 3.38$  J/m), which can be attributed to the more flexible structure of polyurethane resin, already discussed above, and illustrated on Figure 2, enhancing the amount of impact energy the ASG-PU could bear before it breaks. All tested specimens were ruptured in the notch as per the standard and were split into two parts after the impact test.

### 3.7. Energy Dispersive X-ray Spectroscopy (EDS) and Elemental Mapping

To characterize ESG's surface in terms of chemical composition, polished specimens were analyzed with the Energy Dispersive X-ray Spectroscopy (EDS) and Elemental Mapping.

The SEM-EDS chemical analysis with elemental mapping was performed on the polished surfaces of the specimens in the places indicated by Figure 6a (ASG-PU) and 7a (ASG-EP). Figures 6b and 7b both display EDS spectrum of the analyzed specimens (ASG-PU and ASG-EP, respectively, and Figures 6c-h) and 7 c-h) illustrate the specimens' elemental mapping, with element quantification by weight % are presented in Table 9 (ASG-EP) and 10 (ASG-PU) represents the element quantification by % weight

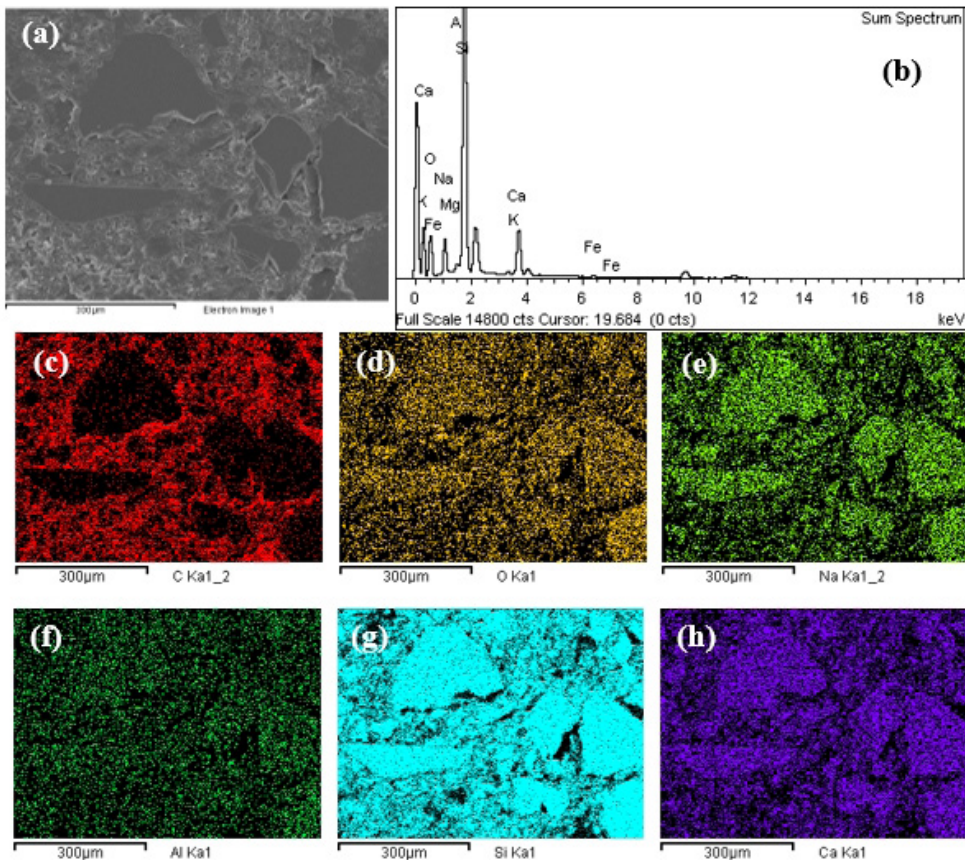


**Figure 6.** SEM-EDS micrographs of polished surface (a), EDS spectrum (b) and corresponding elements maps of C (c), O (d), Na (e), Al (f), Si (g), Ca (h) of ASG-PU.

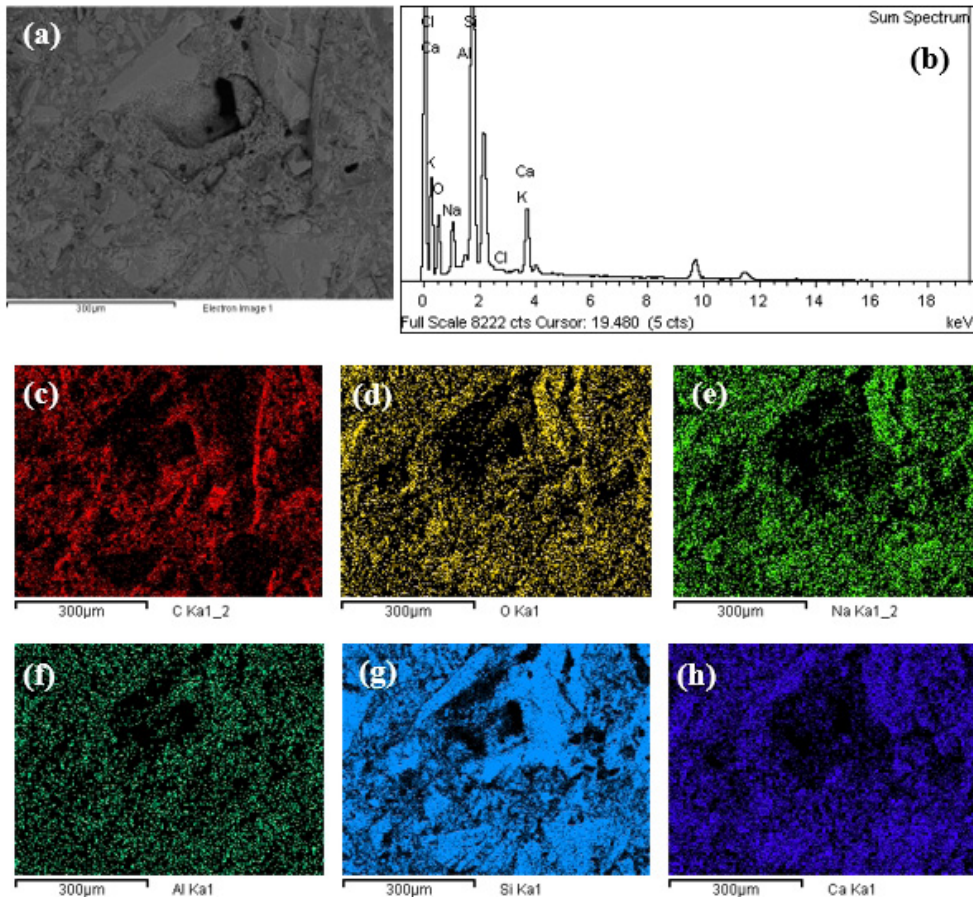


**Figure 7.** SEM-EDS micrographs of polished surface (a), EDS spectrum (b) and corresponding elements maps of C (c), O (d), Na (e), Al (f), Si (g), Ca (h) of ASG-EP.

**Table 9.** EDS element quantification (% weight) of ASG-PU.

Si	O	Ca	Na	Al	K	Fe	Mg
46.91	33.50	10.52	7.07	0.89	0.55	0.37	0.19

**Table 10.** EDS element quantification (% weight) of ASG-EP.

Si	O	Ca	Na	Al	K	Cl
49.21	32.81	10.10	6.34	0.76	0.52	0.25

It is demonstrated through both EDS spectrums that there is an outstanding presence of silicon (Si), oxygen (O), calcium (Ca), and sodium (Na), with was already expected, as they are the primary chemical oxide compositions of waste glass in general ( $\text{SiO}_2$ ,  $\text{NaO}_2$  and  $\text{CaO}$ ), as shown in XRF analysis performed on the waste glass from bottles.

For both ASG, silicon content (light blue) was the highest, followed by oxygen (yellow), calcium (dark blue), and sodium (light green), as shown in Figures 6 and 7.

Tables 9 and 10 present the quantification of elements in weight % of ASG-PU and ASG-EP, respectively. It's worth noticing the differences between them: in the composition of ASG-PU there is a presence of iron (Fe) and magnesium (Mg)

in smaller amounts, while ASG-EP does not present those elements, but presents chlorine (Cl) in its composition. It can be attributed to the resins since ASG-PU and ASG-EP are developed with different matrices, polyurethane, and epoxy.

#### 4. Conclusions

The results found for ASG were mostly in accordance with similar materials proving its technical feasibility, with adequate properties for application in civil construction projects.

A novel engineered stone was developed based on waste glass via vacuum, vibration, and compression method, agglomerated by PU and EP resins.

Best packing composition tests, as well as the definition of the void volume and minimum amount of resin defined the composition of the particles and matrix to develop the artificial stones.

Plates were manufactured with 85% wt. of a waste glass particle mixture, represented by 1/3 coarse, 1/3 medium, and 1/3 fine particles, and with 15%wt of resins, epoxy for ASG-EP and polyurethane for ASG-PU.

Characterization revealed that ASG-PU has 2.14 ( $\pm$  0.01) g/cm<sup>3</sup> density, 0.88 ( $\pm$  0.12)% water absorption, and 1.89 ( $\pm$  0.24)% apparent porosity. ASG-EP has 2.14 ( $\pm$  0.01) g/cm<sup>3</sup> density, 0.74 ( $\pm$  0.01) % water absorption, and 1.59 ( $\pm$  0.01) % apparent porosity. The density results were in accordance with those found by other authors that developed artificial stones with wastes. On the other hand, water absorption and apparent porosity were slightly above those found by other authors, classifying both artificial stones developed as medium-quality coating materials, being suitable to be applied in places with not-so-frequent wetting.

Regarding mechanical resistance, ASG-PU and ASG-EP presented 29.23 and 37.61 MPa, respectively, classifying both as high-quality materials for coating applications according to the technological parameters for artificial and dimensional stones, proving the material's feasibility in the civil construction industry.

ASG-PU's bend strength is lower than ASG-EP which was attributed to influence of the matrix into bending strength, once epoxy resin possesses bend strength of 93.6MPa, higher than polyurethane resin, with 23MPa.

The SEM micrographs of the fractured of bend-ruptured specimens showed low incidence of pores, corroborating the physical indexes results, as well as a great wetting, evidenced by the waste/resin interfacial interaction, corroborating the bend strength results.

Thickness reduction after wear resistance type Amsler test was 2.87( $\pm$ 0.14) mm and 2.15( $\pm$ 0.21) mm for ESG-PU and ESG-EP, respectively, classifying both developed stones, according to Chiodi e Rodriguez, as engineered stones for to be used in floor subjected to medium traffic.

The impact resistance of ASG-PU (14.53 $\pm$ 4.20 J/m) was slightly higher than the impact resistance of ASG-EP (12.70  $\pm$  3.38 J/m), which was attributed to the influence of the matrix in impact resistance. The polyurethane resin is more flexible than epoxy resin, meaning that the stone developed with PU could bear more impact energy before the rupture than the one developed with EP.

The development of artificial stones based on waste glass from bottles and polyurethane and epoxy resins could lead to environmental advantages, such as minimizing waste disposal, and economic advantages, such as diminishing the costs of artificial stones production once it demands expensive aggregates, that in this work were replaced by the waste glass from bottles.

Both ASG-EP and ASG-PU are technically feasible to be applied as civil construction materials.

## 5. Acknowledgments

The authors would like to thank UENF and Universidad de Antioquia, as well as the Brazilian funding agencies, FAPERJ

(process numbers: E-26/200.177/2021, E-26/200.139/2022 and E-26/200.847/2021] and CNPq [process number 302976/2022-1]. This study was also financed in part by the Coordenação de Aperfeiçoamento de Pessoal de Nível Superior – Brasil (CAPES) – Finance Code 001, process number: 88881.690219/2022-01).

## 6. References

- Vinti G, Bauza V, Clasen T, Tudor T, Zurbrügg C, Vaccari M. Health risks of solid waste management practices in rural Ghana: A semi-quantitative approach toward a solid waste safety plan. *Environ Res.* 2023;216(3):114728. <http://dx.doi.org/10.1016/j.envres.2022.114728>.
- Ke J, Cai K, Yuan W, Li J, Song Q. Promoting solid waste management and disposal through contingent valuation method: a review. *J Clean Prod.* 2022;379(1):134696. <http://dx.doi.org/10.1016/j.jclepro.2022.134696>.
- Cordon HCF, Felipe Cagnoni FC, Ferreira FF. Comparison of physical and mechanical properties of civil construction plaster and recycled waste gypsum from São Paulo, Brazil. *J Build Eng.* 2019;22:504-12. <http://dx.doi.org/10.1016/j.job.2019.01.010>.
- Barreto GNS, Babisk MP, Delaqua GCG, Gadioli MCB, Vieira CMF. Evaluation of the effect of the incorporation of blends of fuel and fluxing wastes in red clay ceramics. *Mater Res.* 2019;22(1, Suppl 1):e20190199. <http://dx.doi.org/10.1590/1980-5373-mr-2019-0199>.
- Aguar MCD, Gadioli MCB, Sant'Ana MAK, Almeida KMD, Vidal FWH, Vieira CMF. Red ceramics produced with primary processing fine waste of ornamental stones according to the circular economy model. *Sustainability.* 2022;14(19):12887. <http://dx.doi.org/10.3390/su141912887>.
- Azevedo MC, Marvila MT, Delaqua GCG, Amaral LF, Colorado HA, Vieira CMF. Economy analysis of the implementation of extruded tiles fabrication in a ceramic industry containing ornamental rock waste. *Int J Appl Ceram Technol.* 2021;18(6):1876-90. <http://dx.doi.org/10.1111/ijac.13728>.
- Zulcão R, Calmon JL, Rebello TA, Vieira DR. Life cycle assessment of the ornamental stone processing waste use in cement-based building materials. *Constr Build Mater.* 2020;257:119523. <http://dx.doi.org/10.1016/j.conbuildmat.2020.119523>.
- Prabhu RS, Anuradha R, Jude AB. Understanding the mining waste as resources in self-compacting concrete: a numerical study on sustainable construction. *Resour Policy.* 2022;78:102806. <http://dx.doi.org/10.1016/j.resourpol.2022.102806>.
- Palanisamy C, Velusamy S, Krishnaswami N, Manickam K, Rathinasamy L, Annamalai I. Experimental investigation on self-compacting concrete with waste marble and granite as fine aggregate. *Mater Today Proc.* 2022;65(2):1900-7. <http://dx.doi.org/10.1016/j.matpr.2022.05.159>.
- Gomes VR, Babisk MP, Vieira CMF, Sampaio JA, Vidal FWH, Gadioli MCB. Ornamental stone wastes as an alternate raw material for soda-lime glass manufacturing. *Mater Lett.* 2020;269:127579. <http://dx.doi.org/10.1016/j.matlet.2020.127579>.
- Lakhani R, Kumar R, Tomar P. Utilization of stone waste in the development of value added products: a state of the art review. *J Eng Sci Technol Rev.* 2014;7(3):180-7. <http://dx.doi.org/10.25103/jestr.073.29>.
- Lameiras FS, Silva GDL. Methodology to control the influence of processing factors during composite stone fabrication. *REM Rev Escola Minas.* 2015;68(1):69-75. <http://dx.doi.org/10.1590/0370-44672015680208>.
- Zarzuola R, Almoraima GML, Carretero J, Carbú M, Cantoral JM, Mosquera MJ. Development of a novel engineered stone containing a CuO/SiO<sub>2</sub> nanocomposite matrix with biocidal properties. *Constr Build Mater.* 2021;303:124459. <http://dx.doi.org/10.1016/j.conbuildmat.2021.124459>.

14. Barreto GNS, Carvalho EAS, Souza VS, Gomes M, Azevedo ARG, Monteiro SN, et al. Engineered stone produced with glass packaging waste, quartz powder, and epoxy resin. *Sustainability*. 2022;14(12):7227. <http://dx.doi.org/10.3390/su14127227>.
15. Carvalho EAS, Vilela NF, Monteiro SN, Vieira CMF, Silva LC. Novel artificial ornamental stone developed with quarry waste in epoxy composite. *Mater Res*. 2018;21(1, Suppl 1):e20171104. <http://dx.doi.org/10.1590/1980-5373-mr-2017-1104>.
16. Bagherpor Z, Nazari S, Bagherzadeh P, Fazlavi A. Description and effective parameters determination of the production process of fine-grained artificial stone from waste silica. *SN Appl. Sci*. 2019;1(11):1458. <http://dx.doi.org/10.1007/s42452-019-1491-3>.
17. Erfan NA. Recycling of marble calcite waste into useful artificial marble. *J Adv Eng Trends*. 2021;40(1):6-13. <http://dx.doi.org/10.21608/jaet.2021.82182>.
18. Gomes MLPM, Carvalho EAS, Barreto GNS, Rodriguez RJS, Monteiro SN, Vieira CMF. Development of sustainable artificial stone using granite waste and biodegradable polyurethane from castor oil. *Sustainability (Basel)*. 2022;14(11):6380. <http://dx.doi.org/10.3390/su14116380>.
19. ABNT: Associação Brasileira de Normas Técnicas. ABNT NBR MB 3388: soil: determination of minimum index void ratio of cohesionless soils: method of test. Rio de Janeiro: ABNT; 1991 [cited 2022 Nov 20]. Available from: <https://www.abntcatalogo.com.br/>
20. Peixoto J, Carvalho EAS, Gomes MLPM, Guimarães RS, Monteiro SN, Azevedo ARG, et al. Incorporation of industrial glass waste into polymeric resin to develop artificial stones for civil construction. *Arab J Sci Eng*. 2022;47(4):4313-22. <http://dx.doi.org/10.1007/s13369-021-06071-y>.
21. ABNT: Associação Brasileira de Normas Técnicas. ABNT NBR 15845-2: rocks for cladding. part 2: determination of bulk density, apparent porosity and water absorption. Rio de Janeiro: ABNT; 2015 [cited 2022 Nov 10]. Available from: <https://www.abntcatalogo.com.br/>
22. ABNT: Associação Brasileira de Normas Técnicas. ABNT NBR 15845-6: rocks for cladding. Part 6: determination of modulus of rupture (three point bending). Rio de Janeiro: ABNT; 2015 [cited 2022 Nov 10]. Available from: <https://www.abntcatalogo.com.br/>
23. ABNT: Associação Brasileira de Normas Técnicas. ABNT NBR 12042: inorganic materials: determination of the resistance to abrasion. Rio de Janeiro: ABNT; 2012 [cited 2022 Nov 10]. Available from: <https://www.abntcatalogo.com.br/>
24. ASTM: American Society for Testing and Materials. ASTM D256: standard test methods for determining the izod pendulum impact resistance of plastics. West Conshohocken: ASTM; 2018.
25. Xin Y, Robert D, Mohajerani A, Tran P, Pramanik BK. Transformation of waste-contaminated glass dust in sustainable fired clay bricks. *Case Studies in Construction Materials*. 2023;18:e01717. <http://dx.doi.org/10.1016/j.cscm.2022.e01717>.
26. Arias-Eraza J, Villaquirán-Cacedo MA, Goyes CE. Ecological light transmitting concrete made from glass waste and acrylic sheets. *Constr Build Mater*. 2021;304:124644. <http://dx.doi.org/10.1016/j.conbuildmat.2021.124644>.
27. Ahmed H. Characteristics of micro and nano composite from marble and granite wastes. *Int J Thin Film Sci Technol*. 2021;10(3):4.
28. Lee MY, Ko CH, Chang FC, Lo SL, Lin JD, Shan MY, et al. Artificial stone slab production using waste glass, stone fragments, and vacuum vibratory compaction. *Cement Concr Compos*. 2008;30(7):583-7. <http://dx.doi.org/10.1016/j.cemconcomp.2008.03.004>.
29. Agrizzi CP, Carvalho EAS, Gadioli MCB, Barreto GNS, Azevedo ARG, Monteiro SN, et al. Comparison between synthetic and biodegradable polymer matrices on the development of quartzite waste-based artificial stone. *Sustainability*. 2022;14(11):6388. <http://dx.doi.org/10.3390/su14116388>.
30. Chiodi C Fo, Rodrigues EP. Guide application of stone coverings [Internet]. Brasília: ABIROCHAS; 2020. 232 p. [cited 2022 Dec 13]. Available from: <https://abirochas.com.br/ebooks/bula/#p=5>
31. Debnath S, Ranade R, Wunder SL, Mccool J, Boberick K, Baran G. Interface effects on mechanical properties of particle-reinforced composites. *Dent Mater*. 2004;20(7):677-86. <http://dx.doi.org/10.1016/j.dental.2003.12.001>.
32. ASTM: American Society for Testing and Materials. ASTM C880: standard test method for flexural strength of dimension stone. West Conshohocken: ASTM; 1998.
33. Miller JD, Ishida H, Maurer FHJ. Dynamic-mechanical properties of interfacially modified glass sphere filled polyethylene. *Rheol Acta*. 1988;27(4):397-404. <http://dx.doi.org/10.1007/BF01332160>.
34. Rajalakshmi P, Marie JM, Maria Xavier AJ. Castor oil-derived monomer ricinoleic acid based biodegradable unsaturated polyesters. *Polym Degrad Stabil*. 2019;170:109016. <http://dx.doi.org/10.1016/j.polymdegradstab.2019.109016>.
35. Ansari AA, Kamil M. Izod impact and hardness properties of 3D printed lightweight CF-reinforced PLA composites using design of experiment. *In J Lightweight Mater Manuf*. 2022;5(3):369-83. <http://dx.doi.org/10.1016/j.ijlmm.2022.04.006>.